Thermal Science and Engineering Progress 13 (2019) 100363

Contents lists available at ScienceDirect

Thermal Science and Engineering Progress

journal homepage: www.elsevier.com/locate/tsep

Thermal modeling of deep borehole heat exchangers for geothermal applications in densely populated urban areas

Stefano Morchio, Marco Fossa*

DIME Dept., University of Genova, Italy

ARTICLE INFO

Keywords:
Ground coupled heat pumps
Coaxial pipe geometry
Deep borehole heat exchanger

ABSTRACT

Ground coupled heat pumps are known as very energy efficient heating and cooling systems for a variety of building applications. In densely populated areas where new urbanization is intense, deep ground heat exchangers can be a valuable and effective solution for geothermal heat pump applications. In this paper a finite difference numerical model has been developed starting from literature contributions by Holmberg et al. (2016). The in house Fortran90 code has been built and validated to cope with variable longitudinal and radial mesh distribution for simulating coaxial pipe configurations. Different ground properties and geothermal gradients can be applied. Far field boundary conditions, ground pipe meshing and Courant numbers have been varied for enhancing the accuracy in predicting the fluid temperature evolution. The model has been extensively validated against analytical solutions and literature data. The model has been applied for analyzing the behavior of deep heat exchangers in the 500–800 m range and the effects of the pipe diameter ratio have been investigated both in terms of fluid temperature evolution and pressure losses inside inner and annular pipes.

1. Introduction

Several models for the analysis of the thermal behavior of coaxial vertical heat exchangers have been developed in last years. They are employed in heat pump geothermal applications (Ground Coupled Heat Pumps, GCHP) as well as for the analysis of experimental data in Thermal Response Test (TRT) measurements. Coaxial heat exchangers are triggering great interest in the Scandinavian countries (e.g. the Swedish Effsys program, Mazzotti et al. [1]) for a variety of positive features. These vertical coaxial exchangers can be also installed at depths larger than the conventional borehole heat exchangers (BHE) and when they overcome some 350 m (typical limit for air drilling) are referred to as deep borehole heat exchangers (DBHE). Drilling at very high depth (even to 800–1000 m) has the great advantage of exploiting higher temperature levels and thus more favorable heat transfer conditions. For instance, it has been proven that a 800 m long Deep BHE is capable of achieving the heat transfer guaranteed by 6 or more *U* conventional heat exchangers, each having a length of 300 m (Holmberg et al. [2]). In such a way the surface extension for drilling is reduced together with the total pipe length. These aspects make the deep boreholes particularly suitable to be employed in those areas where lack of land is a constraint, as in towns where there is a high density of buildings associated with a high level of heat demand. These towns can be characterized by vast surfaces already occupied by geothermal low/medium length traditional installations, as it happens in many suburbs of large Swedish cities. The high thermal load assured by a single DBHE together with high coefficient of performance (COP) and the limited CO_2 emissions make this type of application a valid energy solution for many cold, densely populated regions.

To summarize, deep BHEs exploit the favorable temperatures of ground at high depth and help reducing the land use at surface. While considering the benefits that can be obtained by adopting this solution, typical higher costs (and technical complications) associated to drilling at such depths, must be considered.

The use of the DBHEs in the Geothermal Heat Pump industry can contribute to energy savings and emission reduction in densely populated areas like, for example, many Chinese regions.

Regarding the specific case of China, geothermal heat pumps had a great development in this Country and in recent years GCHP installations had a progressive annual increase rate of over 27%; Ground Source Heat Pump (GSHP) application has reached 330 million m^2 in China in 2014 (Zheng et al. [3]). Cities like Beijing, Tianjin and Shenyang have established a series of GSHP systems, which led to a massive reduction of CO_2 emissions of 19.87×10^6 tons (Zhang and Hu [4]).

BHEs and their deep counterparts can be also employed as interface

* Corresponding author.
E-mail address: marco.fossa@unige.it (M. Fossa).

https://doi.org/10.1016/j.tsep.2019.100363
Received 15 April 2019; Received in revised form 28 May 2019; Accepted 31 May 2019

Nomenclature

A	Area [m^2]
c	specific heat [J/kg·K]
COP	coefficient of performance [–]
Co	Courant number [–]
E_1	exponential integral in ILS model [–]
Fo	Fourier number [–]
G	temperature transfer function [–]
g	multi BHE temperature transfer function [–]
h	heat transfer coefficient [W/m^2·K]
H	active depth of the BHE [m]
k	thermal conductivity [W/(m·K)]
$\dot{m}$	mass flow rate [kg/s]
$\dot{Q}$	heat transfer rate [W]
$\dot{Q}'$	heat transfer rate per unit length [W/m]
R	thermal resistance [m·K/W]
r	radial coordinate [m]
T	temperature [K]
t	time [s]
V	volume [m^3]
w	velocity [m/s]
z	vertical coordinate [m]

Greek letters

α	thermal diffusivity [m^2/s]
ρ	density [kg/m^3]
Δ	finite increment in a variable [–]

Subscripts

a	annular pipe
b	borehole
c	center pipe
f	heat carrier fluid
$f1$	heat carrier fluid in the annular pipe
$f2$	heat carrier fluid in the center pipe
gr	of the ground medium, of the ground domain
i	index, spatial discretization (radial)
j	index, spatial discretization (vertical)
m	membrane (outer pipe)
n	index, temporal discretization
w	water
∞	far field and initial condition

for seasonal solar thermal energy storage. Gao et al. [5] reviewed the studies on borehole seasonal solar thermal energy storage. They considered analytical and numerical models for ground thermal recharge and carried system simulations. They showed that in the specific case of China, there are still some special problems for the development of borehole seasonal solar thermal storage, the key problems being related to the lack of land and a quite slow development in building integrated solar collectors.

The effective use of GCHPs is mainly related to the correct modeling and simulation of ground heat exchangers and their surrounding ground volume. This is particularly important for deep BHEs and coaxial ones. The approaches for predicting the heat exchanger behavior are typically of three types and they can be classified in semi-analytical models, thermal resistance and capacitance models, finite difference (or volumes) methods.

Semi-analytical models are described in the next section and they refer to the base analytical solutions of the Fourier conduction equation. Carslaw and Jaeger [6] contributed to the solution of the cylindrical heat source, Ingersoll et al. [7] presented the Infinite line source problem, Eskilson [8] first solved the problem of the thermal response of a system of linear sources arranged in a given geometry. More recent contributions are those by Cimmino and Bernier [9] that solved the Eskilson problem by applying analytical solutions to segments of the linear source and by Priarone and Fossa [10] that compared the single line source response at different boundary conditions. Capacity Resistance Models (CRM) solve a system where unknowns are ground and BHE thermal capacitances and resistances and they are particularly suitable for short to medium term simulations (De Carli et al. [11], Bauer et al. [12], Zarrella et al. [13]).

In the present investigation a hybrid method based on both the concept of thermal resistances and finite difference has been developed and applied for simulating long coaxial BHEs according to the approach recently proposed by Holmberg et al. [2]. This study is stressing some issues related to model validation and proper spatial and temporal discretization and it is applied to demonstrate how hydraulic optimization and heat transfer from ground can be properly simulated for short to medium time analyses.

2. Theoretical background on coaxial ground heat exchangers

Thermal conduction in the ground is one of the fundamentals hypotheses used in thermal response models for geothermal heat exchangers analysis. Carslaw and Jaeger [6] first provided the ground theoretical response of single heat sources pertaining to the Infinite Line Source (ILS) category. This infinite linear source does not have a dimension in the radial direction and it extends in an infinite medium. A constant and uniform specific heat transfer rate is applied to the ground:

$$T(r,\tau) - T_{gr,\infty} = \frac{\dot{Q}'}{4\pi k_{gr}} \int_{\frac{1}{4Fo_r}}^{\infty} \frac{e^{-\beta}}{\beta} d\beta = \frac{\dot{Q}'}{4\pi k_{gr}} E_1(1/4Fo_r) \tag{1}$$

The ILS model provides the ground temperature $T(r,\tau)$ as a function of the radial distance and time. Here k_{gr} is the ground thermal conductivity, $T_{gr,\infty}$ is the undisturbed ground temperature, Fo_r is the radius based Fourier number and finally E_1 is the exponential integral function, which has a very useful expression as expansion series:

$$E_1(x) = -\gamma - \ln(x) - \sum_{n=1}^{m} \frac{(-1)^n x^n}{n n!} \tag{2}$$

here x = $1/4Fo_r$ and γ is the Euler constant (γ ≈ 0.5772). E_1 can also be approximated by the Abramowitz and Stegun formulas [14]:

$$0 \le x \le 1$$
$$E_1(x) = a_0 - \ln(x) + a_1 x + a_2 x^2 + a_3 x^3 + a_4 x^4 + a_5 x^5 + \varepsilon(x)$$
$$|\varepsilon(x)| < 2 * 10^{-7} \tag{3}$$

$$a_0 = -0.57721566 \quad a_1 = 0.99999193 \quad a_2 = -0.24991055$$

$$a_3 = 0.05519968 \quad a_4 = -0.00976004 \quad a_5 = 0.00107857$$

$$1 \le x < \infty$$
$$E_1(x) = (x^2 + b_1 x + b_2)/[x e^x (x^2 + b_3 x + b_4)] + \varepsilon(x)$$
$$|\varepsilon(x)| < 5 * 10^{-5} \tag{4}$$

$$b_1 = 2.334733 \quad b_2 = 0.250621 \quad b_3 = 3.330657 \quad b_4 = 1.681534$$

It can be demonstrated that Eq. (3) is also accurate within 1% at Fo_r higher than 0.145 (Fossa [15]) and both Eqs. (3) and (4) are much more accurate than the typical E_1 approximation employed since Mogensen pioneering work [16].

Another one-dimensional model (and solution) available for infinite ground medium is the Infinite Cylindrical Source (ICS) model, by Ingersoll et al. [7]. Compared to the ILS model, the specific heat transfer rate (per unit source length) is applied to the surface of a hollow infinite cylinder of given radius. The solution is described by a rather complex analytical function that was named the "G" one, whose values are often available in tabular form:

$$T(r,\tau) - T_{gr,\infty} = \frac{\dot{Q}'}{k_{gr}} G\left(Fo_{rb}, p = \frac{r}{r_b}\right) = \frac{1}{\pi^2}\int_0^\infty \frac{e^{-\beta^2 \cdot Fo_{rb}} - 1}{J_1^2(\beta) + Y_1^2(\beta)} [J_0(p\beta)Y_1(\beta) - J_1(\beta)Y_0(p\beta)] \frac{1}{\beta^2} d\beta \quad (5)$$

where J_0, J_1, Y_0, Y_1 are Bessel functions of the zeroth and first order, respectively.

More recent semi analytical models have been developed to better describe a real ground heat exchanger located in a semi-finite volume. These models belong to the family of the Finite Line Source (FLS) and the main contribution are by Eskilson [8], Spitler and Yavuzturk [17], Zeng [18], Lamarche and Beauchamp [19], Claesson and Javed [20], Cimmino et al. [21].

Numerical models assume great importance in solving the heat conduction equation in a finite domain. Eskilson [8] had defined new temperature transfer functions (Temperature Response Factor) known as g-functions:

$$T_{ave}(r_b) - T_{gr,\infty} = \frac{\dot{Q}'_{ave}}{2\pi k_{gr}} g(\ln(9Fo_H),\ r_b/H,\ B/H,\ \ borefield\ geometry) \quad (6)$$

The g-function is calculated by using numerical or semi-analytical methods (according to different boundary conditions as discussed by Cimmino and Bernier [9] and Priarone and Fossa [10])). Often g-functions are available graphically (as reported in Eskilson Doctoral Thesis [8]). The dimensionless g-solutions provide the performance of a borehole for various borefield geometries.

Line and cylindrical source models, briefly discussed above, do not describe the pipe geometry of the BHE and further inner BHE models have been proposed to this aim. Hellstrom [22] suggested that the coaxial geometry may have some advantages in reducing borehole thermal resistance. Beier et al. [23] focused on the coaxial design, in particular on the pipe-in-pipe geometry. Zanchini et al. [24] studied a coaxial design in which the stainless steel outer pipe is in direct contact with the surrounding ground. Acuña and Palm [25] described a coaxial pipe in which an external flexible tube filled with water pushes the conduit against the borehole wall. Beyond this, Acuña [26] measured the fluid and borehole wall vertical temperature profile in a coaxial heat exchanger during a Distributed TRT (DTRT experiment). It has been demonstrated by Acuña [27] that coaxial exchangers exhibit better thermal performance when compared to traditional *U* pipes. From the hydrodynamic point of view, considering the same operating conditions and the same drilling dimension, the coaxial heat exchanger has a reduced total pressure loss when compared to *U* pipes because of its larger hydraulic diameter.

De Carli et al. [11] proposed a model based on electric analogy (Capacity Resistance Model, CaRM) for vertical heat exchangers (Coaxial pipe, single U-pipe, double U-pipe). Bauer et al. [12] developed two-dimensional thermal resistance and capacity models (TRCM) for different types of BHE (coaxial included); these models consider the thermal capacity of the grouting material. Furthermore, the coaxial geometry is used to correctly locate the center of the grout thermal capacity for single-U and double-U geometries. A similar model configuration can also be found in Beier and Smith [28]. Beier et al. [23] developed an analytical model to predict vertical temperature profiles of the circulating fluid in a coaxial heat exchanger (pipe-in-pipe geometry). This model handles an arbitrary vertical temperature profile in the undisturbed ground; the heat transfer between the fluid within the BHE and the surrounding ground is represented by using a thermal resistance model.

Holmberg et al. [2] developed a numerical model that employs both thermal resistances and the finite difference scheme in the ground medium for simulating coaxial BHE response and assessing the overall performance in terms of total COP, including the energy requirements in the circulation pumps.

Iry and Rafee [29], have performed numerical simulations with a commercial CFD code changing the ratio between the diameters of a coaxial BHE having a length up to 165 m. Fang et al. [30] have stated that the operation of DBHEs combined with heat pumps seems more appropriate and economically sustainable for building heating. They also studied the effect of central pipe insulation. Their studies indicate that an insulated inner pipe makes significant difference in DBHE performance due to its mitigation of thermal short-circuiting between the upward and downward-flowing fluids.

3. Present model for the coaxial ground heat exchanger

Studies related to the coaxial DBHE, able to cope with non-constant ground properties and possibly with peculiar ground temperature profiles are a quite new research activity. The present approach to a detailed description of the behavior of a long coaxial heat exchanger is made by developing a two-dimensional axisymmetric model based on the finite difference approach coupled by a thermal resistance description of the pipe wall effects. This numerical model solves the transient conduction and convection problem inside the heat exchanger and in the surrounding ground by imposing a given (constant or not) heat transfer rate to the carried fluid at the top inlet section of the heat exchanger. A Fortran90 program has been built and it is an evolution of the model proposed by Holmberg et al. [2]. In the present model, the mesh describing the thermal volumes is variable along the radial as well as the longitudinal direction. The contributions to Holmberg et al.

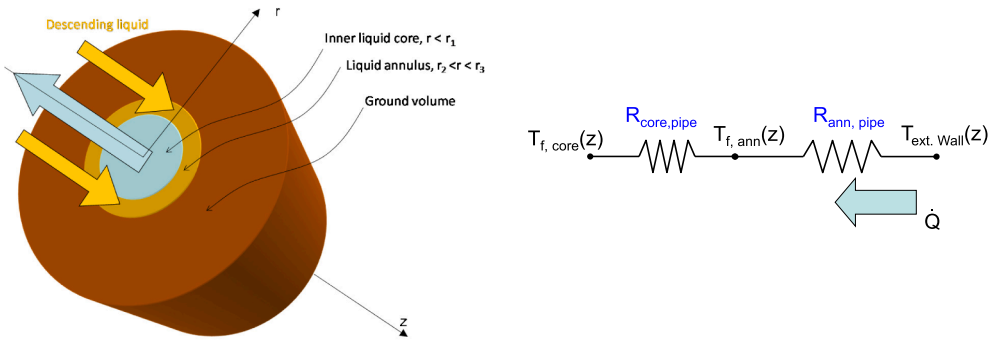

Fig. 1. Axisymmetric geometry and thermal resistance network.

model are several: they include an analysis on Courant number effects, a proposed criterion for selecting the correct radial mesh spacing and distribution based on the ILS analytical solution, further comparisons and parametric analyses.

The ground thermo-physical properties as well as the geothermal gradient (i.e. the undisturbed ground temperature profile) can change along the vertical z axis and non-conventional temperature distributions can be taken into account. Worth noticing, for deep heat exchangers it is quite likely that such anomalous ground temperature distributions can be found in real installations and their anomalies can affect the overall performance of the heat pump. This aspect can hardly be accounted for using an analytical model (e.g. the ILS or FLS ones).

Time step, heat load, fluid mass flow rate, heat load variation in time can be set depending on the simulation targets. The numerical problem solution may be obtained using two different far field boundary conditions, namely an undisturbed temperature profile (as a function of z) or an adiabatic boundary condition (BC). By comparing the numerical results from both BCs it is possible to establish the correct dominion extension, and this is an additional contribution to the present paper to this problem. The present model has been validated by using theoretical data and temperature profiles related to a 490 m DBHE coaxial heat exchanger. Further simulations then are here performed by both changing the diameters of the coaxial pipes as well as the undisturbed ground temperatures.

3.1. Model assumptions and equation set

The electro-thermal analogy has been conveniently used to describe the inner pipe and fluid heat transfer through proper thermal resistances (Fig. 1). The numerical grid (Fig. 2) implements a two-dimensional axial-symmetric model in cylindrical geometry. An upwind energy balance is applied to fluid volumes and the finite difference discretization of the Fourier equation is applied to the ground volume. The thermal inertia of pipes is neglected.

The total thermal resistance $R_{core,pipe}$ between the geothermal fluid in the central pipe and the fluid in the annular pipe is expressed by the following equation:

$$R_{core,pipe} = \frac{1}{2\pi r_1 h_c} + \frac{\ln\left(\frac{r_2}{r_1}\right)}{2\pi k_c} + \frac{1}{2\pi r_2 h_a} \tag{7}$$

Fluid direction can be also reverted with respect to the above representation. Pipe thickness is not present in the sketch.

The total thermal resistance $R_{ann,pipe}$ between the carrier fluid in the annular conduit and the borehole wall surface is expressed by the following equation:

$$R_{ann,pipe} = \frac{1}{2\pi r_3 h_a} + \frac{\ln\left(\frac{r_4}{r_3}\right)}{2\pi k_m} + \frac{\ln\left(\frac{r_b}{r_4}\right)}{2\pi k_w} \tag{8}$$

The above equation considers the possibility that a thin (quiet) water film (k_w conductivity) is present in between the outer pipe and the rock medium; in such a way any different contact resistance can be taken into account. The convective heat transfer coefficients are calculated using the Petukhov correlation in the Gnielinski [31] version. The bulk fluid velocity w is calculated by the mass flow rate and pipe diameters assumed as inputs for the problem solution.

The convective heat transfer coefficient inside the annular duct is assumed to be the same on both the outer and inner walls, since it is expected that their maximum difference is within 5% (Kays et al. [32]).

The thermal conduction in the ground surrounding the borehole is expressed by the Fourier law in cylindrical coordinates, in the absence of internal heat generation:

$$\frac{1}{r}\frac{\partial}{\partial r}\left(rk_g\frac{\partial T}{\partial r}\right) + \frac{\partial}{\partial z}\left(k_g\frac{\partial T}{\partial z}\right) = \rho c\frac{\partial T}{\partial t} \tag{9}$$

Eq. (9) is discretized by introducing a numerical grid based on finite difference. It consists of nodes along the radial direction r (indexed with the letter i) and along the axial direction z (indexed with the letter j). In general, a variable internodal spacing along r and along the z directions can be assumed. Variable thermo-physical properties along z can be considered and set and for this reason the ground thermal diffusivity α_j and the ground thermal conductivity k_j are here indexed with the letter j.

By applying the transient energy conservation law to each control volume, it is possible to write the finite difference formulation of the two-dimensional thermal conduction equation for each ground node as follows:

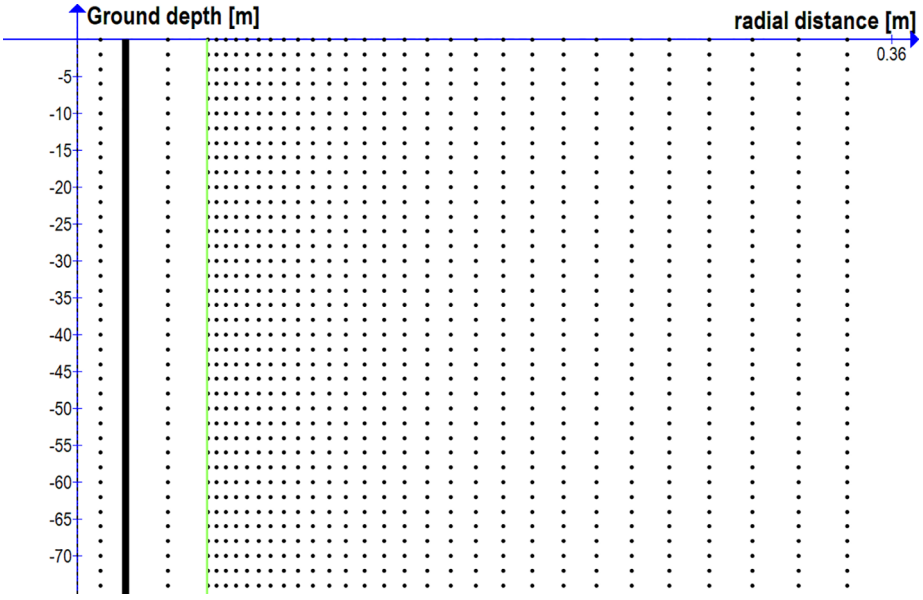

Fig. 2. Node distribution along the radial and vertical directions for a given portion of the calculation domain. Nodes left of solid lines represent liquid volumes.

$$\frac{T_{i,j}^{n+1} - T_{i,j}^{n}}{\Delta t} = \left(\frac{2\alpha_j}{r_i \Delta r_i}\right)[AT_{i+1,j}^{n+1} - (A+B)T_{i,j}^{n+1} + T_{i-1,j}^{n+1}B] + \frac{(2\alpha_{j+1})}{\Delta z_j}\frac{(T_{i,j+1}^{n+1} - T_{i,j}^{n+1})}{\Delta z_j + \Delta z_{j+1}} - \frac{(2\alpha_j)}{\Delta z_j}\frac{(T_{i,j}^{n+1} - T_{i,j-1}^{n+1})}{\Delta z_j + \Delta z_{j-1}} \quad (10)$$

The terms A and B group the following quantities:

$$A = \frac{\left(r_i + \frac{\Delta r_i}{2}\right)}{\Delta r_i + \Delta r_{i+1}} \quad (11)$$

$$B = \frac{\left(r_i - \frac{\Delta r_i}{2}\right)}{\Delta r_i + \Delta r_{i-1}} \quad (12)$$

The expression (10) follows an implicit scheme. It is also possible (depending on the choices made by the user) to maintain an evenly spaced grid along z and/or along r. Present simulations have been carried out with a non-constant radial grid, while depth distances have been uniformly spaced.

Proper z spacing has been chosen by comparing the fluid temperature results in the first 10 h (the most affected by grid issues) by doubling the finite volumes in the depth direction with respect to the reference grid (100 partitions along z). The maximum fluid temperature difference resulted to be 0.2 K (for any instant and volume position) and the average one less than 0.02 K.

Interdistances between radial nodes have been selected following the "intrinsic log" nature of the heat diffusion as suggested by the ILS analytical solution. For this reason, the following radial distribution law has been applied:

$$r_{i+1} = r_i e^{deltaprecision\left(\frac{2\pi k_{gr}}{\dot{Q}'}\right)} \quad (13)$$

This law has been here derived from the ILS analytical equation (it has been considered the expansion series of the exponential integral function truncated at the second term) where *deltaprecision* is to some extent related to the temperature difference between two adjacent nodes. This parameter can be selected as an input as a tradeoff between reduced round off errors and node overall number. The presence to the $k_{gr}/\dot{Q}'$ ratio comes from the ILS solution itself and it is related to the temperature gradients in the radial direction, to be properly managed with a suitable radial mesh.

Fig. 2 shows the node distribution along z and r, where each node is identified by its coordinates. The solid lines identify the cylindrical axisymmetric surfaces of pipes.

The following energy balance equations describe the thermal transient of each fluid control volume within the BHE. In the equations below, ΔT is the carrier fluid temperature difference at pipe top inlet and outlet.

In the following, the discretization schemes in the annular pipe, center pipe, inlet and outlet top nodes outside ground, respectively, are provided.

$$\frac{({T_{f1,j}}^{n+1} - {T_{f1,j}}^{n})}{\Delta t} = \frac{w_{f1}({T_{f1,j-1}}^{n+1} - {T_{f1,j}}^{n+1})}{\Delta z_j} + \frac{({T_{1,j}}^{n+1} - {T_{f1,j}}^{n+1})}{\rho c \pi ({r_3}^2 - {r_2}^2) R_{ann,pipe}} + \frac{({T_{f2,j}}^{n+1} - {T_{f1,j}}^{n+1})}{\rho c \pi ({r_3}^2 - {r_2}^2) R_{core,pipe}} \quad (14)$$

$$\frac{({T_{f2,j}}^{n+1} - {T_{f2,j}}^{n})}{\Delta t} = \frac{w_{f2}({T_{f2,j+1}}^{n+1} - {T_{f2,j}}^{n+1})}{\Delta z_j} + \frac{({T_{f1,j}}^{n+1} - {T_{f2,j}}^{n+1})}{\rho c \pi {r_1}^2 R_{core,pipe}} \quad (15)$$

$$\frac{(T_{f1,j}^{n+1} - T_{f1,j}^{n})}{\Delta t} = \frac{w_{f1}(T_{f2,j}^{n+1} + \Delta T - T_{f1,j}^{n+1})}{\Delta z_j} \quad (16)$$

$$\Delta T = \frac{\dot{Q}}{\dot{m}c} \quad (17)$$

$$\frac{(T_{f2,j}^{n+1} - T_{f2,j}^{n})}{\Delta t} = \frac{w_{f2}(T_{f2,j+1}^{n+1} - T_{f2,j}^{n+1})}{\Delta z_j} \quad (18)$$

Similar equations have been written for the case when the fluid enters from the top of the central pipe (descending fluid in central pipe).

The conductive heat transfer in the ground equals the one transferred through the overall thermal resistance $R_{ann,\ pipe}$ of the BHE:

$$(T_{f1,j} - T_{1,j})\frac{\Delta z_j}{R_{ann,pipe}} = -\frac{k_j 2\pi r_b \Delta z_j (T_{2,j} - T_{0,j})}{(\Delta r_1 + \frac{\Delta r_0}{2} + \frac{\Delta r_2}{2})} \quad (19)$$

From Eq. (19) it is possible to write the following Eq. (20), valid for the borehole wall nodes:

$$\frac{T_{1,j}^{n+1} - T_{1,j}^{n}}{\Delta t} = \left(\frac{2\alpha_j}{r_1 \Delta r_b}\right)\left[(A+B)T_{2,j}^{n+1} - (A+B)T_{1,j}^{n+1} + ({T_{f1,j}}^{n+1} - {T_{1,j}}^{n+1})\frac{(\Delta r_1 + \frac{\Delta r_0}{2} + \frac{\Delta r_2}{2})}{R_{ann,pipe} k_j 2\pi r_b}B\right] + \frac{(2\alpha_{j+1})}{\Delta z_j}\frac{(T_{1,j+1}^{n+1} - T_{1,j}^{n+1})}{\Delta z_j + \Delta z_{j+1}} - \frac{(2\alpha_j)}{\Delta z_j}\frac{(T_{1,j}^{n+1} - T_{1,j-1}^{n+1})}{\Delta z_j + \Delta z_{j-1}} \quad (20)$$

Far field boundary condition can be applied with either given temperature T_{gr} (z) profile or adiabatic modes. Proper grid sizing and dominion extension can be checked by applying both the boundary conditions (BCs) and cross checking the numerical results.

$$\text{Initial condition: } t = 0; \quad T(r, z, 0) = T_{gr}(z) \quad (21)$$

$$\text{Boundary condition (type 1)} \begin{cases} T(r, 0, t) = T_{gr}(0)\ \forall\ r \geq r_b \\ T(r_{\max}, z, t) = T_{gr}(z) \\ \frac{\partial T(r,z,t)}{\partial z}\Big|_{z=z_{\max}} = 0 \end{cases} \quad (22)$$

$$\text{Boundary condition (type 2)} \begin{cases} T(r, 0, t) = T_{gr}(0)\ \forall\ r \geq r_b \\ \frac{\partial T(r,z,t)}{\partial r}\Big|_{r=r_{\max}} = 0 \\ \frac{\partial T(r,z,t)}{\partial z}\Big|_{z=z_{\max}} = 0 \end{cases} \quad (23)$$

Eqs. (10) to (23) constitute a system that can be written in matrix form which has been here solved by applying an iterative Gauss Seidel algorithm.

Grid spacing and time steps have been carefully evaluated by assessing the effects of different Courant numbers *Co* on the results of the simulations.

$$Co = \frac{w\Delta t}{\Delta z} \quad (24)$$

The *Co* analysis has been carried out for a specific test case described by Table 1 data.

A constant ground temperature gradient has been considered, as can be found for example in Italian litologies, even for deep boreholes (e.g. Della Vedova et al. [33]). Courant numbers have been changed in the 0.2 to 1 range, until fluid temperatures (especially in the first 10 h of simulation) did not differ as an average for more than 0.1 °C and as a maximum difference for more than 0.2 °C. Fig. 3 shows as an example the effects of the different Courant numbers in the very hearly period (t = 0.46 and 0.92 h) and in the late one (t = 92 h). The present

Table 1
Model validation: BHE geometry and operating conditions for 800 m BHE.

Borehole length	800 m
Borehole diameter	0.140 m
Center pipe diameter	0.09 m
Center pipe thickness	0.008 m
Annular pipe diameter	0.139 m
Annular pipe thickness	0.0004 m
Mass flow rate	3 kg/s
Heat load	32,000 W
Fluid inlet pipe	Inner pipe
Ground thermal conductivity	3 W/mK
Ground thermal diffusivity	10^{-6} m^2/s
Geothermal gradient	0.02 K/m

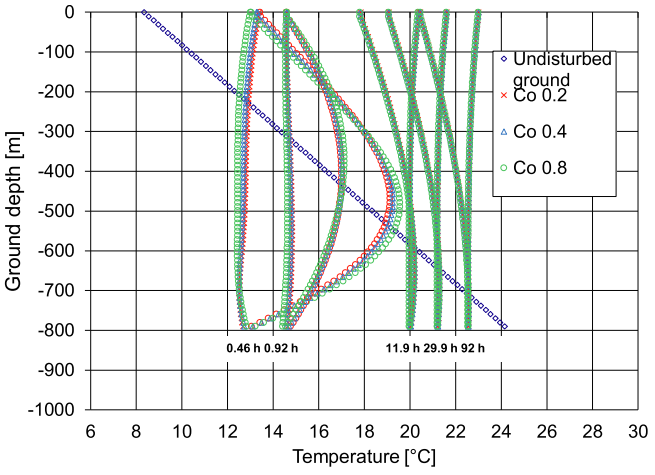

Fig. 3. Fluid temperature profiles for a long BHE (800 m) as a function of time and different Courant numbers when the undisturbed ground temperature profile is linear with depth.

analysis suggested that Courant number equal to 0.4 seems suitable for assuring accuracy while saving at most the computational time.

4. Model validation against theoretical solutions

A preliminary series of calculations (with BC types 1 and 2) have been carried out with reference to a DBHE 800 m long. The length of the BHE has been selected for both stressing the model capability to cope with very deep heat exchangers and to simulate conditions like the ones related to the ILS model. In such a way, even if the simulation is carried out by considering the fluid circulation, the ground temperature distribution (at mid BHE depth, where end effects are expected to be negligible) can be compared with ILS 1D predictions. The geometry and operating conditions of this first reference case are provided in Table 1.

Two BC conditions (adiabatic or given temperature at outer ground radius) have been applied for checking that the overall ground volume is large enough for describing the far field persistency of initial temperature profile. The two solutions (at different BC) show an excellent agreement and the related values are within a thousandth of degree (Fig. 4). More important, they show a trend at the end time (T(r) traced for $r_b \le r \le r_{max}$ and for $z = H/2$ at 90 h) that follows the trend predicted by the ILS model using the Abramowitz and Stegun formulas.

Further simulations have been carried for retracing some operating conditions considered in Holmberg et al. [2] paper. Table 2 describes this specific case and the related geometry. The BHE is 490 m long and the time span is 50 h, simulating a TRT in heat extraction mode (or a winter operating condition for a heat pump).

Fig. 5a shows the literature temperature profiles while Fig. 5b shows the present model predictions in terms of fluid temperatures (inner pipe and annular one) and BHE wall. In both figures the undisturbed ground temperature profile (input of simulation) is reported together with the calculated local heat transfer rate (per unit length). As can be observed the agreement is good and the present model is able to well replicate the reference data.

Table 2
Model comparison with literature data: BHE geometry and operating conditions for 490 m BHE.

Borehole length	490 m
Borehole diameter	0.140 m
Center pipe diameter	0.05 m
Center pipe thickness	0.0046 m
Annular pipe diameter	0.139 m
Annular pipe thickness	0.0004 m
Mass flow rate	1 kg/s
Heat load	−19,600 W
Fluid inlet pipe	Annular pipe
Ground thermal conductivity	3.53 W/mK
Ground thermal diffusivity	10^{-6} m^2/s

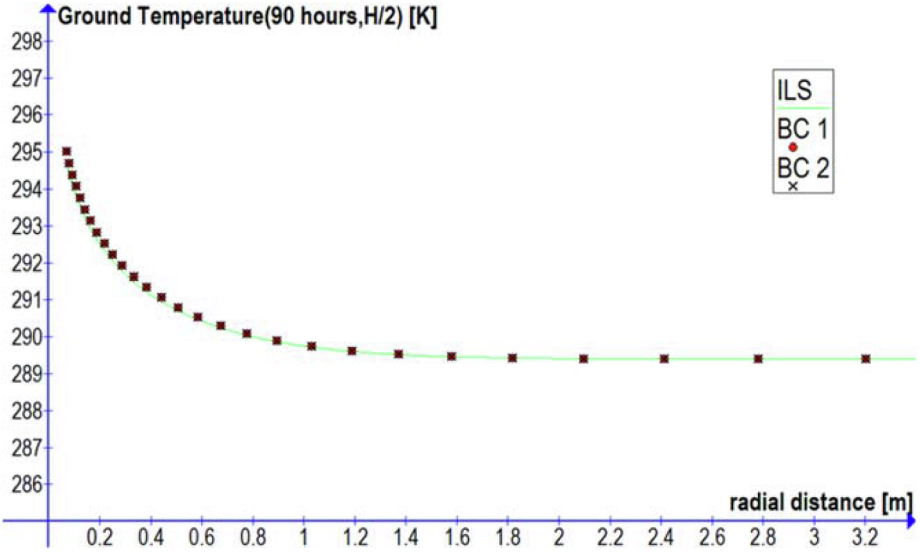

Fig. 4. Radial temperature in the ground medium at mid BHE depth after 90 h of heat injection and comparison with ILS predictions at same Fo number. Different BC conditions at external radius are applied.

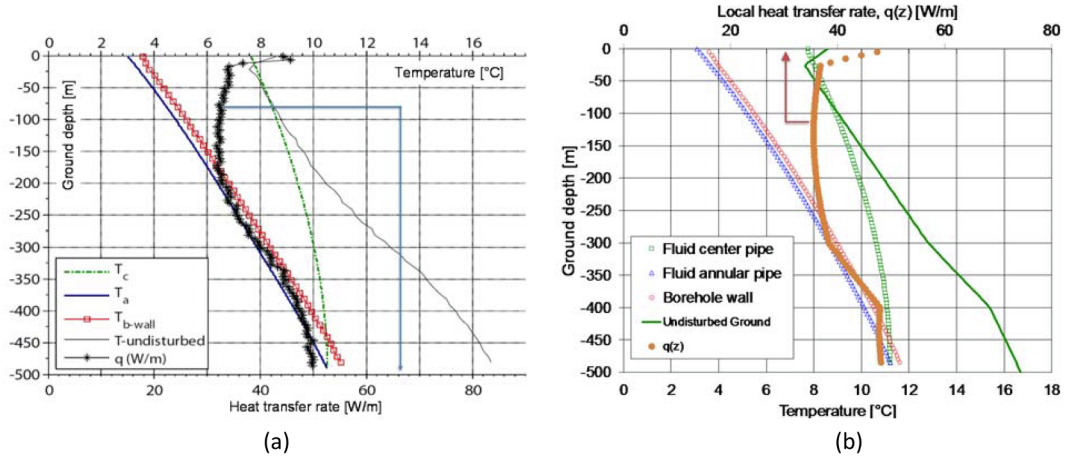

Fig. 5. Fluid and BHE temperatures along the z-axis (depth) as reported in Holmberg et al. [2] paper (left) and as calculated with the present model (right). Time is 50 h.

Table 3
Parametric analysis data: pipe geometry and flow rates.

Test Case #	Center Pipe inner diameter [m]	Mass flow rate [kg/s]	Center Pipe wall thickness [m]
1	0.05	3	0.008
2	0.075	3	0.008
3	0.085	3	0.008
4	0.09	3	0.008
5	0.1	3	0.008
6	0.105	3	0.008
7	0.08	3	0.008
8	0.08	3.5	0.006
9	0.08	3.5	0.002

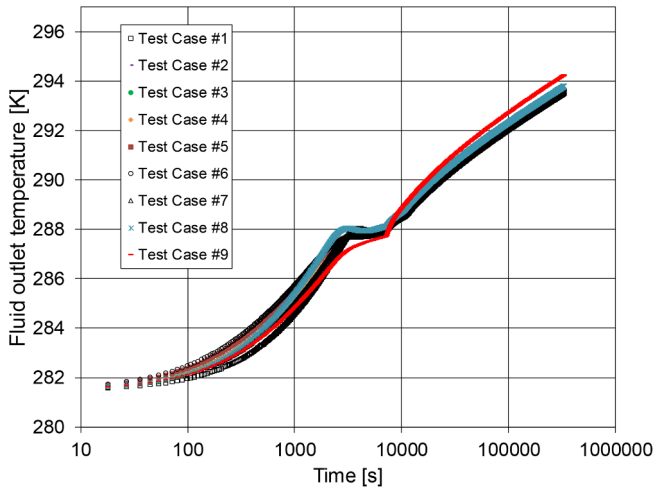

Fig. 6. Temperature of the fluid leaving the BHE over time, for different coaxial pipe geometries.

5. Results and discussion

One of the objectives of the present investigation was to obtain indications on hydrodynamic and thermal performance of such DBHES for general design purposes. Attention is paid to the temperature of the fluid exiting the borehole and to the pressure losses experienced by the fluid inside pipes at a given mass flow rate. Different simulations have been carried out while changing the diameter ratios of the coaxial heat exchanger. Simulations refer to 9 geometries with a time horizon of about 100 h. Even if the model can be applied for longer time windows (tuning the ground outer diameter accordingly), the above duration has

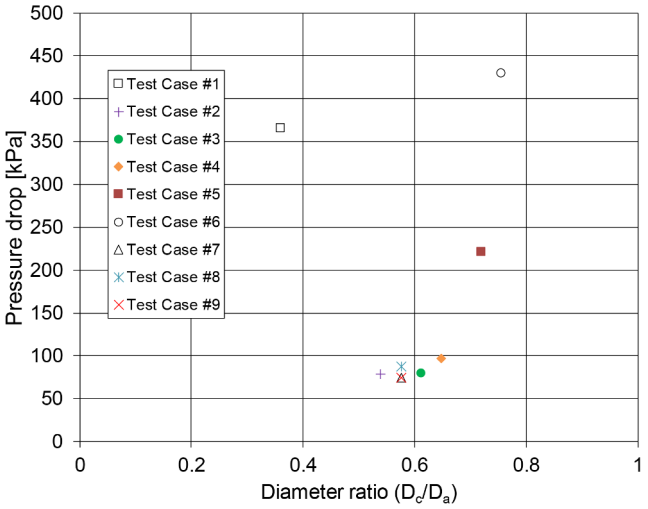

Fig. 7. Pressure drop in coaxial pipes for Table 3 operating conditions as a function of the inner to annular pipe diameter ratios.

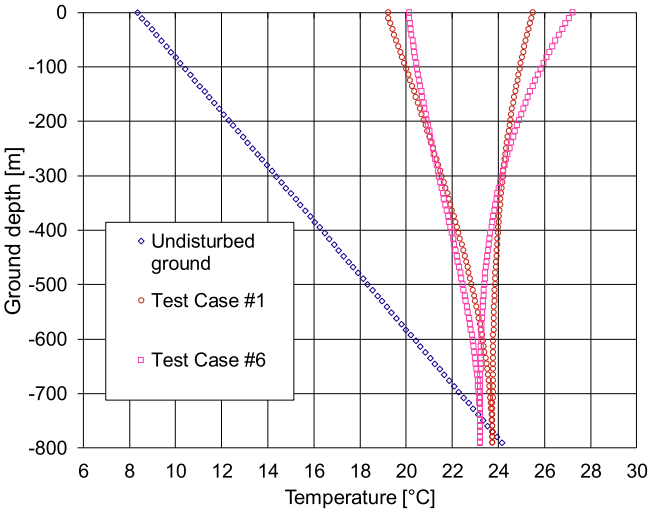

Fig. 8. Fluid and ground temperature profiles at the end of a 92 h period of constant heat injection in the ground. Mass flow rate is tuned for yielding the same pressure drop in the different pipe geometries. Cases #1 and #6 are considered as extreme conditions.

been considered suitable for both describing the hydraulic issues related to coaxial boreholes and obtaining useful information related to thermal effects during the heat load peak periods, ranging from fraction of hours to few days. Worth noticing, the 100 h range is also suitable for describing the on/off cycles of the heat pump in order to apply, by superposition techniques, the present short term DBHE response to the long term one, as calculated from g-function models. DBHE dimensions are those described in Table 1 and just the diameter ratios have been changed according to Table 3 parameters. The mass flow rate of the carrier fluid is increased for the test #8 and test # 9, while the center pipe wall thickness is reduced compared to the other tests.

Fig. 6 shows the exit fluid temperature from BHE and the pipe geometry is the parameter. Worth noticing, the lower is the exit temperature the better is the heat exchanger performance. The first 7 tests (which differ only for the different diameter of the central pipe) involve temperatures at the outlet of BHE, which remain all within about 0.15 K. There is an initial thermal transient related with the first two hours of circulation of the flow without supplying heat. Test #8 differs on average by about 0.30 K in terms of BHE outlet temperature compared to Test #1. Test #9 has slightly larger temperature differences (0.65 K) compared to case #1. The lowest outlet temperature, all along time, is obtained by geometry #1 having a diameter of central pipe equal to 0.05 m (the diameter of the annular pipe is set to 0.139 m for all nine cases).

Fig. 7 refers to pressure losses due to pipe friction and shows an interesting profile passing through a minimum at a diameter ratio (Center pipe over annular one) located at about 0.55–0.60. This result is in close agreement with the findings by Iry and Rafee [29], according to whom the minimum pumping power in a 165 m coaxial BHE can be achieved at a diameter ratio of 0.65. The above diameter ratio range thus seems to represent the optimum choice for reducing the pumping power at a given flow rate.

In the present investigation, also taking into account the similar thermal performance of all BHEs, geometries #7 to #9 seem to be the best ones from both thermal and hydrodynamic point of view.

A final series of simulations have been carried out by imposing the overall pressure drop related to geometry #7 (about 75 kPa) to all the other heat exchangers by varying their mass flow rates. In such a way the new flow rates range from 1.0 kg/s (geometry #6) to 3.0 kg/s (geometry #7). It can be noticed that imposing the pressure loss is equivalent to work with a pump at given head.

Fig. 8 shows the fluid temperatures along the DBHE at the final instant of the simulations (92 h) for different coaxial pipe diameter ratios. Fig. 8 also shows the far field (and initial) ground temperature which varies linearly (as an assumption for these simulations) with depth due to a constant geothermal gradient.

It can be noticed that, at common heat transfer rate for all geometries, the inlet/outlet temperature difference $\Delta T_{in/out}$ changes with mass flow rate. Consequently, the increase of $\Delta T_{in/out}$ moves the fluid temperatures near the heat exchanger bottom in the direction of the undisturbed (initial) temperature, thus producing a “temperature inversion” between fluid and ground. In addition to “temperature inversion” effects, the different pipe geometry plays the role of controlling the “thermal short circuiting” between the descending liquid in the inner pipe and the rising liquid inside the annulus. The comparison for example of cases #6 and #1 having more or less the same mass flow rate but larger inner pipe diameter for case #6, is particularly interesting. Cases #1 and #6 are here selected and represented in Fig. 8 since they represent the two extreme conditions among the geometries here considered. Geometry #6 has a higher heat transfer area (pipe to pipe) with respect to case #1 and this situation enhances the short circuiting, carrying the descending fluid #6 (inside the inner pipe) to a lower temperature at BHE bottom with respect to fluid in pipe #1. On the other hand, the rising #1 fluid can be better cooled by the surrounding ground without being heated too much by its descending counterpart, thus gaining an outlet temperature at BHE top section lower than the case #6 one.

6. Conclusions

In this paper a finite difference model, implemented in a Fortran 90 calculation program, has been developed for studying the thermal performance of deep coaxial boreholes for geothermal applications in densely built urban areas. The model has been tuned in terms of proper grid and time step characterization to accurately describe the fluid and ground temperature evolution along the radius and the depth of the heat exchanger. Criteria for both the Courant number and radial grid spacing criteria have been proposed and validated. Contributions to the reference model by Holmberg et al. paper have been provided and the present results and conclusion are consistent with the above reference study. The attention was focused on the early period (100 h) of heat exchanger response, the most important for describing the on/off cycles of the heat pump and its peak working conditions. Simulations have been performed for different pipe geometries while maintaining the same borehole external diameter to assess the geometry effects on fluid friction losses and fluid temperature along the heat exchanger and the inlet and outlet sections at the heat pump side. Concerning the combined effect on pressure drop and best temperatures, an optimum diameter ratio (inner to annular pipe) belonging to the 0.5–0.6 range has been found for a given linear distribution of ground undisturbed temperatures. Further investigations and applications of the present model will be related to the effects of the geothermal gradient anomalies and on the direction of the carrier fluid in the coaxial pipes.

Declaration of Competing Interest

None.

References

[1] W. Mazzotti, J. Acuña, A. Lazzarotto, B. Palm, Deep Boreholes for Ground Source Heat Pump, Final Report Effsys Expand (Energimyndigheten), KTH (Sweden), 2018, pp. 1–77.
[2] H. Holmberg, J. Acuña, E. Næss, O.K. Sønju, Thermal evaluation of coaxial deep borehole heat exchangers, Renew. Energy 97 (2016) 65–76.
[3] K. Zheng, Y. Mo, L. Chen, Twenty years of geothermal heat pumps in China, Proceedings World Geothermal Congress 2015, (2015).
[4] X. Zhang, Q. Hu, Development of geothermal resources in China: a review, J. Earth Sci. 29 (2) (2018) 452–467, https://doi.org/10.1007/s12583-018-0838-9.
[5] L. Gao, J. Zhao, Z. Tang, A review on borehole seasonal solar thermal energy storage, Energy Procedia 70 (2015) 209–218, https://doi.org/10.1016/j.egypro.2015.02.117.
[6] H.S. Carslaw, J.C. Jaeger, Conduction of Heat in Solids, Claremore Press, Oxford, U.K., 1947.
[7] L.R. Ingersoll, O.J. Zobel, A.C. Ingersoll, Heat Conduction with Engineering, Geological, and Other Applications, McGraw-Hill, New York, 1954.
[8] P. Eskilson, Thermal Analysis of Heat Extraction Boreholes, Ph.D. Thesis Lund University of Technology, Sweden, 1987.
[9] M. Cimmino, M. Bernier, A semi-analytical method to generate g-functions for geothermal bore fields, Int. J. Heat Mass Transfer 70 (2014) 641–650.
[10] A. Priarone, M. Fossa, Modelling the ground volume for numerically generating single borehole heat exchanger response factors according to the cylindrical source approach, Geothermics 58 (2015) 32–38.
[11] M. De Carli, M. Tonon, A. Zarrella, R. Zecchin, A computational capacity resistance model (CaRM) for vertical ground-coupled heat exchangers, Renew. Energy 35 (2010) 1537–1550.
[12] D. Bauer, W. Heidemann, H. Müller-Steinhagen, H.-J.G. Diersch, Thermal resistance and capacity models for borehole heat exchangers, Int. J. Energy Res. 35 (2011) 312–320.
[13] A. Zarrella, M. Scarpa, M. De Carli, Short time step analysis of vertical ground-coupled heat exchangers: the approach of CaRM, Renew. Energy 36 (2011) 2357–2367.
[14] M. Abramovitz, I. Stegun, Handbook of Mathematical Functions with Formulas, Graphs, and Mathematical Tables, Nat. Bureau of Standards, 1964, pp. 228–233.
[15] M. Fossa, Correct design of vertical borehole heat exchanger systems through the improvement of the ASHRAE method, Science and Technology for the Built Environment, Taylor and Francis Inc., 2016, pp. 1080–1089.
[16] P. Mogensen, Fluid to duct wall heat transfer in duct system heat storages, Doc.-Swedish Counc. Build. Res. 16 (1983) 652–657.
[17] C. Yavuzturk, J.D. Spitler, A short time step response factor model for vertical ground loop heat exchangers, Ashrae Trans. 105 (1999) 475–485.
[18] H.Y. Zeng, N.R. Diao, Z.H. Fang, A finite line-source model for boreholes in geothermal heat exchangers, Heat Transfer-Asian Res. 31 (2002) 558–567.
[19] L. Lamarche, B. Beauchamp, A new contribution to the finite Line-source model for

geothermal boreholes, Energy Build. 39 (2007) 188–198.
[20] J. Claesson, S. Javed, An analytical method to calculate borehole fluid temperatures for time-scales from minutes to decades, ASHRAE Trans. 117 (2) (2011) 279–288.
[21] M. Cimmino, M. Bernier, F. Adams, A contribution towards the determination of g-functions using the finite line source, Appl. Therm. Eng. 51 (2013) 1–2.
[22] G. Hellstrom, Borehole Heat Exchangers: State of the Art 2001. Implementing Agreement on Energy Conservation through Energy Storage: Annex 13-Design, Construction and Maintenance of UTES Wells and Boreholes. Subtask 2, International Energy Agency (IEA), 2002.
[23] R.A. Beier, J. Acuña, P. Mogensen, B. Palm, Borehole resistance and vertical temperature profiles in coaxial borehole heat exchangers, Appl. Energy 102 (2013) 665–675.
[24] E. Zanchini, S. Lazzari, A. Priarone, Effects of flow direction and thermal short circuiting on the performance of small coaxial ground heat exchangers, Renew. Energy 35 (2010) 1255–1265.
[25] J. Acuña, B. Palm, First experiences with coaxial borehole heat exchangers, Sources/Sinks Alternative to the Outside Air for Heat Pump and Air-Conditioning Techniques, (2011).
[26] J. Acuña, Improvements of U-pipe Borehole Heat Exchanger, Licentiate Thesis in Energy Technology, KTH, Stockholm, 2010.
[27] J. Acuña, Distributed Thermal Response Tests-New Insights on U-tube and Coaxial Heat Exchangers in Groundwater-filled Boreholes (Doctoral thesis), KTH, Stockholm, 2013.
[28] R.A. Beier, M. Smith, Minimum duration of in-situ tests on vertical boreholes, ASHRAE Trans. 109 (2) (2003) 475–486.
[29] S. Iry, R. Rafee, Transient numerical simulation of the coaxial borehole heat exchanger with the different diameters ratio, Geothermics 77 (2019) 158–165, https://doi.org/10.1016/j.geothermics.2018.09.009.
[30] L. Fang, N. Diao, Z. Shao, K. Zhu, Z. Fang, A computationally efficient numerical model for heat transfer simulation of deep borehole heat exchangers, Energy Build. 167 (2018) 79–88.
[31] V. Gnielinski, New equations for heat and mass transfer in turbulent pipe and channel flow, Int. Chem. Eng. 16 (1976) 359–368.
[32] W. Kays, M. Crawford, B. Weigand, 2005, Convective Heat and Mass Transfer.
[33] B. Della Vedova, B. Petronio, F. Poletto, F. Palmieri, A. Marcon, B. Farina, A. Cimolino, C. Bellezza, The geothermal district heating system on the Grado Island (North-eastern Adriatic Sea), Proceedings World Geothermal Congress 2015, Melbourne, Australia, 19–25 April 2015, 2015, pp. 1–12.